ORIGINAL ARTICLE

Comprehensive Transcriptome Analysis of Tea Crabapple (*Malus hupehensis* Rehd.) Roots Subjected to Mixed Saline–Alkali Stress

Xin-Liang Wang[1,2] · Ling Peng[2] · Jian Wang[1] · Jing-Jing Jia[1] · Li-Ping Tang[1]

Abstract

Soil salinization–alkalization is a major hindrance to agricultural development globally. Tea crabapple is widely used in China. However, little remains known regarding the molecular mechanisms used to withstand mixed saline–alkali stress (MSAS). Herein, we exposed tea crabapple seedlings to MSAS, and RNA-seq was performed for the transcriptome analysis of roots. Between 43.26 million and 43.37 million clean reads were thus obtained. In comparison with the control group (day 0), 2931, 2335, and 3746 genes were differentially expressed at day 1, day 3, and day 6 of MSAS exposure, respectively, and 1022 genes were common in the three comparison groups. On functional annotation, we observed that numerous differentially expressed genes were involved in "global and overview maps"; "carbohydrate metabolism"; "folding, sorting, and degradation"; "biosynthesis of other secondary metabolites"; "environmental adaptation"; and "signal transduction." Heat shock proteins, cytochrome P450s, disease-resistant proteins, non-specific lipid-transfer proteins, pectate lyase, and beta-glucosidases were also induced in response to MSAS, in addition to nitrogen, phosphorus, and potassium absorption and metabolism-related genes. Transcription factor-coding genes appear to regulate the response of tea crabapple roots to MSAS by participating in, for example, plant hormone signal transduction and heat shock response. We also performed quantitative real-time PCR to validate the expression of six differentially expressed genes. Our findings provide new insights into the molecular mechanisms used by tea crabapple to cope with MSAS.

Keywords Tea crabapple · Mixed saline–alkali stress · Transcriptome · Transcription factor · Signal transduction

Key Messages

- We studied the response of tea crabapple roots to mixed saline–alkali stress (MSAS).
- One thousand twenty-two overlapping DEGs were identified across three comparison groups.
- Genes encoding various transcription factors significantly responded to MSAS.
- Genes associated with nitrogen, phosphorus, and potassium metabolism regulation facilitate tolerance to MSAS.

✉ Xin-Liang Wang
wiln1@163.com

1 Editorial Department of Journal of Binzhou University, Binzhou University, Binzhou 256603, China

2 Shandong Key Laboratory of Eco-Environmental Science for the Yellow River Delta, Binzhou University, 391 Huanghe 5th RoadShandong Province, Binzhou 256603, China

Introduction

Soil salinization–alkalization, the predominant environmental factor affecting plant growth, not only makes the soil seriously devoid of nitrogen (N), phosphorus (P), potassium (K), and other minerals but also affects their absorption and metabolism by plants (Ye et al. 2019). Salt stress causes osmotic injury and ion toxicity in plants, whereas alkali stress exposes them to high pH levels. On subjecting *Medicago ruthenica* seedlings to mixed saline–alkali stress (MSAS), Yang et al. (2011) observed a significant decrease in photosynthetic characteristics, such as net photosynthetic rate, stomatal conductance, intercellular CO_2 concentration, and chlorophyll content, with an increase in salinity and pH. MSAS is not just a simple superposition of salt and alkali stresses, but there is a certain synergistic effect that causes complex, serious damage to plants. Plants have evolved various complex domestication mechanisms to withstand adverse environmental conditions. Among them, at the molecular level, stress signaling pathways play a critical role in plant

abiotic stress response by linking sensing mechanisms with genetic responses (Khan et al. 2018). Transcription factors (TFs) serve as molecular switches to control gene expression in response to stress, playing a key role in regulating plant adaptation to abiotic stress conditions. Plants possess numerous genes that encode various TFs. For example, *Arabidopsis* has been suggested to have > 1500 such genes, which are classified into > 40 families (Riechmann et al. 2000). In addition to their role in stress response, TFs are involved in, for instance, embryogenesis, plant morphology, and inflorescence development.

Apple (*Malus × domestica* Borkh.) is the fourth largest fruit crop in terms of production and consumption across the world. In 2018, 86.14 million tons of apples were produced globally (FAOSTAT 2020), with China producing 46% of the total quantity. Soil salinization–alkalization in China has markedly restricted the development of the apple industry. Rootstock affects the growth of fruit trees, in addition to the yield and quality of fruits (Sabatino et al. 2018). Therefore, to enhance the development of the apple industry, it is pivotal to study the molecular mechanisms underlying rootstock response and tolerance to MSAS (Wang et al. 2018). In recent years, most studies have focused on elucidating the mechanisms used by plants to deal with either salt stress or alkali stress, with only few exploring MSAS. Moreover, these studies have primarily focused on comprehending the effects of MSAS on herbaceous plants, and only few are based on apple rootstock (Jia et al. 2019). Tea crabapple (*Malus hupehensis* Rehd. var. pingyiensis) is a widely used apple rootstock in China and has the properties of apomixis; therefore, it appears appropriate for molecular research.

In this study, we applied RNA-seq to study the response of tea crabapple seedlings to MSAS at the transcriptomic level. Differentially expressed genes (DEGs), TF-coding genes, and pathways affected upon MSAS exposure were identified. Furthermore, we performed quantitative real-time PCR (qRT-PCR) to identify and analyze the expression patterns of some key response genes. We believe our results should facilitate the breeding of plants that are highly tolerant to MSAS.

Methods

Plant Materials

The experiments were performed at Binzhou University (Shandong Province, China). From January 2020, tea crabapple seeds were sterilized with 0.2% KMnO$_4$ for 30 min and then rinsed in running water. The seeds were stratified in the sand at 4 °C for nearly 60 days. After germination, they were planted in a plastic basin (22 cm × 21 cm) containing a nutrient matrix (3:2:1 volume ratio of sand, vermiculite, and soil). All seedlings were allowed to grow in natural light and temperature

conditions in the outdoor, and half-strength Hoagland nutrient solution (pH = 6.8 ± 0.2) was used for irrigation.

Stress Exposure

The seedlings were divided into the control and treatment (i.e., MSAS) groups. When the seedlings had grown for 43 days, they were 6- to 7-cm tall and had 5–7 true leaves, and they were exposed to MSAS. According to the soil characteristics in the Yellow River Delta, the seedlings were treated with NaCl, Na$_2$SO$_4$, and NaHCO$_3$ (2:1:1 molar ratio of NaCl, Na$_2$SO$_4$, and NaHCO$_3$), and the final concentrations of NaCl, Na$_2$SO$_4$, and NaHCO$_3$ are 100, 50, and 50 mmol/L, respectively. The control group was irrigated with half-strength Hoagland nutrient solution, whereas the MSAS group was irrigated with half-strength Hoagland nutrient solution containing mixed salts (pH = 8). For both groups, new roots were harvested on day 0 (R000), day 1 (R001), day 3 (R003), and day 6 (R006). There were two replicates for R000 and three replicates each for R001, R003, and R006. All samples were stored at − 80 °C for further analyses.

RNA Extraction, Transcriptome Sequencing, and Read Analysis

We used the TRIzol method to extract total RNA from the samples. NanoDrop (Thermo Fisher Scientific Inc., USA) and Agilent 2100 Bioanalyzer (Agilent technology, USA) were used for RNA quality determination. The isolated total RNA was then used to enrich mRNA by oligonucleotide (dT) magnetic beads. Short mRNA fragments were obtained using a fragment buffer and reverse transcribed into double-stranded cDNA with random N6 primers. Specific primers were used for PCR to amplify cDNA fragments. The amplicons thus obtained were purified and thermally denatured into single-stranded DNA. The Agilent 2100 Bioanalyzer was used to evaluate the quality of library, and the BGISEQ-500 platform was used for sequencing.

Raw reads were filtered with Trimmomatic to remove reads with adaptors, unknown base N content greater than 5%, and low quality. Clean reads were then mapped against the reference genome sequence [*Malus × domestica* GDDH13 Whole Genome v1.1 (https://www.rosaceae.org/; Jung et al. 2019)] with Bowtie2 (Langmead et al. 2009), and RSEM was used to calculate the gene expression level of each sample. Gene expression was calculated in terms of fragments per kilobase per million mapped reads.

Analysis of Gene Expression Levels and Functional Annotation

To improve the robustness of DEG identification, we defined genes with log$_2$ (fold change) ≥ 1 or ≤ − 1 and *Q* value (adjusted

P value)≤0.001 as being significantly differentially expressed. Subsequently, DEGs were functionally annotated using the gene ontology (GO) database (http://www.geneontology.org/; The Gene Ontology Consortium 2019), and the Kyoto Encyclopedia of Genes and Genomes (KEGG) database (https://www.genome.jp/kegg/pathway.html) was used to identify the metabolic pathways in which they were involved. Enrichment analyses were performed using the "phyper" function in R, and *P* value and *Q* value were calculated. In general, *Q* value≤0.05 indicated significant enrichment.

qRT-PCR

The expression levels of six DEGs were verified by qRT-PCR. The samples for qRT-PCR and RNA-seq were independent of each other, and each sample had three biological repeats. RNA was extracted using the TRIzol method. First-strand cDNA was synthesized using a RT Reagent Kit with gDNA Eraser (RR047A, Takara), and qRT-PCR was performed with TB Green® Premix Ex Taq™ II (RR820A, Takara). The 10-µL reaction volume contained 5 µL SYBR, 3 µL ddH$_2$O, 1 µL cDNA template, and 0.5 µL forward and reverse primers each. The cycling conditions were as follows: 95 °C for 30 s, followed by 40 cycles of 95 °C for 5 s and 60 °C for 30 s. The elongation factor-1 alpha gene (*EF-1α*) was used the internal reference gene. Table S1 shows primer sequences. Relative gene expression levels were measured using the $2^{-\Delta\Delta CT}$ method.

Results

Sequencing Data

Probably due to the short treatment time, the phenotypes of tea crabapple did not change significantly under MSAS (Fig. 1). Upon performing RNA-seq, each sample produced 43.82 million raw reads, which were then cleaned, as described above. Consequently, between 43.26 million and 43.37 million clean reads were obtained; Q20 was > 96.90% and Q30 was > 91.90% (Table S2). Tables 1, S2–S4 show the results obtained on mapping clean reads against the reference genome using Bowtie2. Approximately 72.37–73.82% clean reads could be mapped to the reference gene; 33.67–34.41% clean reads were uniquely mapped to the reference gene. The number of genes expressed in each sample was > 33,000 and that of novel transcripts was > 1800.

Identification and Functional Annotation of DEGs

We assessed differential gene expression patterns between the control and MSAS groups to identify key genes that were expressed upon exposure to MSAS. In comparison with the control group, after R001 of MSAS exposure, 996 genes were upregulated and 1935 were downregulated; after R003 of MSAS exposure, 895 genes were upregulated and 1440 were downregulated; and after R006 of MSAS exposure, 1054 genes were upregulated and 2692 were downregulated (Fig. 2A). The number of DEGs ranged from 6.79 to 11.08% of total genes. In the three comparison groups (i.e., R001 vs. R000, R003 vs. R000, and R006 vs. R000), the number of common DEGs was 1022, which was approximately 3% of total genes (Fig. 2B). Hierarchical cluster analysis was performed using these common DEGs (Fig. 2C, Table S5), which revealed that upon MSAS exposure, the expression levels of approximately 30% and 70% DEGs were up- and downregulated, respectively.

To identify the biological functions of DEGs, GO enrichment analysis and functional annotation were performed. DEGs were classified into three core categories: biological processes, cellular components, and molecular function. Herein, the 1022 DEGs were enriched in 39 functional groups. In the molecular function category, most DEGs were enriched in "binding" and "catalytic activity"; in the cellular components category, most DEGs were enriched in "membrane" and "membrane part"; and in the biological processes category, most DEGs were enriched in "metabolic process" and "cellular process" (Fig. 3A). The results of GO enrichment analysis are shown in Table S6 (*Q*≤0.05).

Furthermore, KEGG pathway enrichment analysis was performed using the 1022 DEGs (Fig. 3B). KEGG pathways can be divided into five categories: cellular processes, environmental information processing, genetic information processing, metabolism, and organismal systems. We found that a large number of DEGs were involved in "global and overview maps"; "carbohydrate metabolism"; "folding, sorting and degradation"; "biosynthesis of other secondary metabolites"; "environmental adaptation"; and "signal transduction." Table S7 provides information pertaining to significantly enriched KEGG terms (*Q*≤0.05).

Analysis of Genes that Significantly Responded to MSAS

We further analyzed genes that showed a large change in their expression levels [log$_2$ (fold change)≥4 or ≤ −4 in at least one comparison group]. Nucleotide sequences were compared against the NCBI protein database using BLASTx to infer biological functions. We found that the genes encoded several proteins, such as chlorophyll a/b binding proteins, cytochrome P450 (CYP450)-like proteins, lipid-transfer proteins, and TFs (Table 2).

Analysis of Genes Encoding TFs

Our analyses led to the identification of > 30 TF families. Table 3 shows the top 15 TF families that were the most

Fig. 1 Phenotypes of tea crabapple under mixed saline–alkali stress (MSAS)

Table 1 Summary of sequencing results

| Sample	R000	R001	R003	R006
Raw reads (M)	43.82	43.82	43.82	43.82
Clean reads (M)	43.31	43.27	43.26	43.37
Total clean bases (G)	6.50	6.49	6.49	6.51
Clean reads Q20 (%)	97.28	97.22	97.40	97.20
Clean reads Q30 (%)	92.88	92.69	93.18	92.53
Total mapped (%)	31,641,155 (73.07)	31,941,734 (73.82)	31,627,996 (73.11)	31,389,525 (72.37)
Uniquely mapped (%)	34.41	34.35	33.67	33.69
Total number of expressed genes	34,868	34,021	34,410	33,802
Novel transcripts	1942	1857	1916	1828
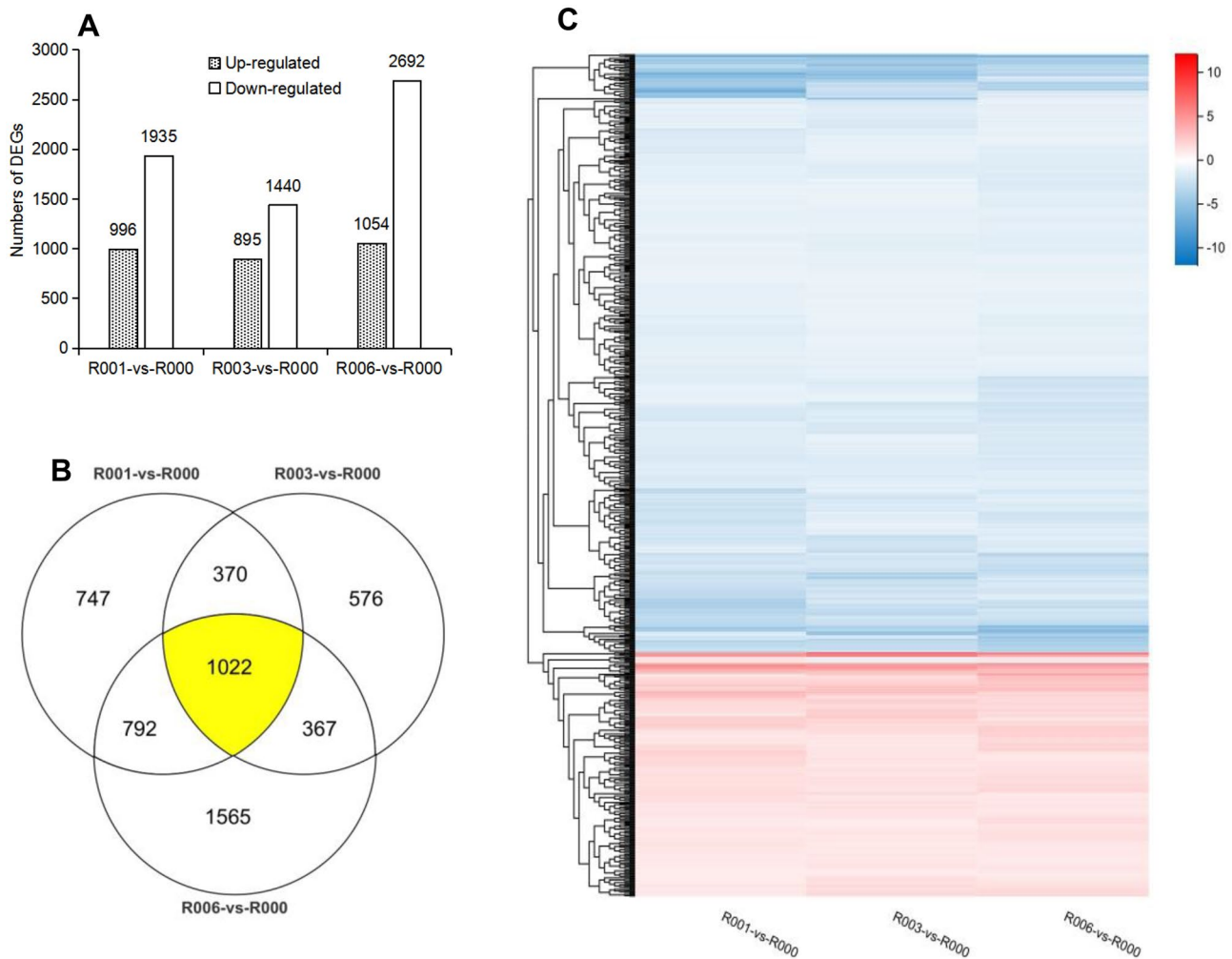
Fig. 2 Differentially expressed genes (DEGs) in tea crabapple roots exposed to MSAS. **A** Numbers of DEGs induced in response to MSAS. **B** Venn diagrams of DEGs in the three comparison groups. **C** Heatmap showing the expression patterns of 1022 common DEGs.

Red and blue indicate genes with up- and downregulated expression levels, respectively. R000: control; R001, R003, and R006: MSAS for 1, 3, and 6 days, respectively

influenced upon MSAS exposure, such as APETALA2/ethylene-responsive element-binding protein (AP2-EREBP), myeloblastosis (MYB), basic helix–loop–helix (bHLH), no apical meristem–Arabidopsis transcription activation factor–cup-shaped cotyledon (NAC), WRKY, and heat stress (or heat shock) TF (HSF). MYB showed the largest number of affected TFs ($n = 329$), followed by AP2-EREBP ($n = 218$), bHLH ($n = 190$), NAC ($n = 173$), WRKY ($n = 120$; containing the signature 60-amino-acid-long WRKY domain that is highly conserved), and Cysteine3Histidine (C3H; $n = 107$). The AP2-EREBP family included the highest number of DEGs, followed by the MYB, bHLH, and NAC families; however, the C2C2-CO-like family had the highest percentage of DEGs (52.94%), followed by the HSF (39.47%) and AP2-EREBP (31.65%) families. In the three comparison groups, MSAS affected the expression

levels of 80 TF-coding genes (Table S8): approximately 33% of them were upregulated and 67% were downregulated (Fig. 4). These 80 TFs belonged to 22 classes, with MYB ($n = 14$), bHLH ($n = 9$), HSF ($n = 7$), and AP2-EREBP ($n = 5$) being the most abundant. GO enrichment analyses revealed that they were mostly enriched in "binding," "cell," and "organelle" (Fig. 5A), and 14 TFs were involved in "regulation of nitrogen compound metabolic process" (Fig. 5B, Table S9).

Genes Involved in N, P, and K Absorption and Metabolism that Were Affected by MSAS

Nitrate transporter (NRT), nitrate reductase (NR), ferredoxin-nitrite reductase (NirA), glutamine synthetase (GS), glutamate synthase (GOGAT), glutamate dehydrogenase (GDH),
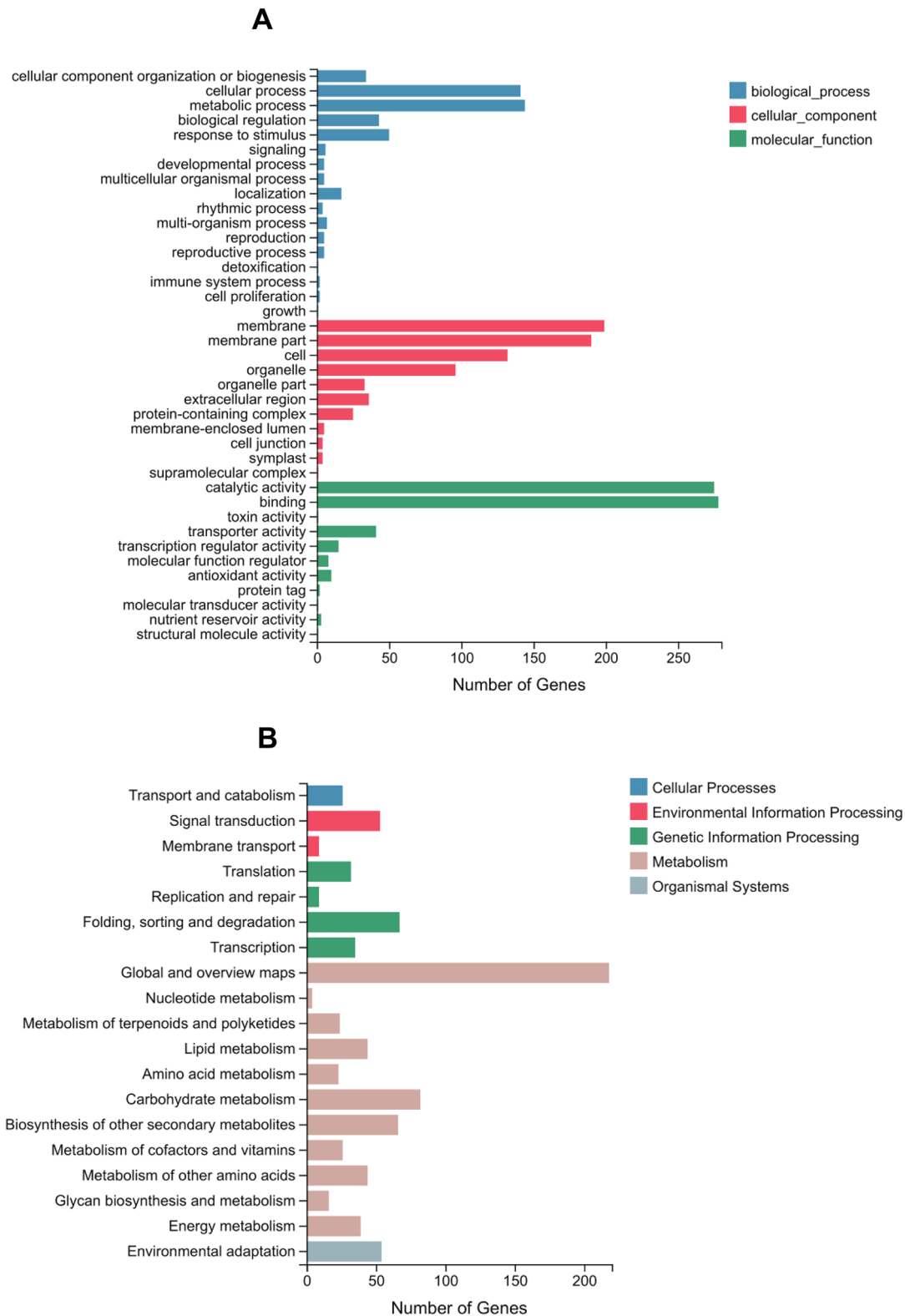
A

B

Fig. 3 Gene ontology (GO) and Kyoto Encyclopedia of Genes and Genomes (KEGG) functional classification of 1022 common DEGs. **A** GO enrichment analysis and functional classification of DEGs. DEGs were enriched in 39 functional groups, which are classified into three categories: biological processes, cellular components, and molecular function. **B** KEGG pathway enrichment analysis and functional classification of DEGs. DEGs were assigned to 19 KEGG pathways. The enrichment analysis divided the 19 pathways into five categories: cellular processes, environmental information processing, genetic information processing, metabolism, organismal systems

Table 2 List of genes with a large change in expression levels [$\log_2$ (fold change) ≥ 4 or ≤ -4 in at least one comparison group]

Gene ID	$\log_2$ (R001/R000)	$\log_2$ (R003/R000)	$\log_2$ (R006/R000)	Search results Match|E value|gene annotation/function
MD04G1148900	6.58	5.50	5.32	XP_008363908.1|3.5e-110|PREDICTED: glycerol-3-phosphate 2-O-acyltransferase 6-like
MD00G1159900	6.57	6.91	6.06	XP_008363530.1|0.0e+00|PREDICTED: putative SWI/SNF-related matrix-associated actin-dependent regulator of chromatin subfamily A member 3-like 1
MD10G1280900	6.27	8.75	5.31	XP_008383634.1|2.1e-239|PREDICTED: U-box domain-containing protein 7-like
MD04G1022700	6.15	5.43	4.37	XP_008382481.1|7.9e-113|PREDICTED: protein SUPPRESSOR OF npr1-1, CONSTITUTIVE 1-like
MD05G1230000	5.89	10.94	6.81	XP_008380474.1|3.1e-141|PREDICTED: adenosylhomocysteinase
MD11G1219700	5.54	7.37	8.59	XP_008364815.1|2.4e-289|PREDICTED: LOW QUALITY PROTEIN: cytochrome P450 CYP736A12-like
MD14G1080000	5.52	5.49	5.90	XP_008351633.1|4.9e-197|PREDICTED: glucan endo-1,3-beta-glucosidase, basic isoform-like
MD11G1021300	5.41	5.40	4.23	XP_008366172.2|2.6e-154|PREDICTED: G-type lectin S-receptor-like serine/threonine-protein kinase LECRK4
MD15G1103700	4.78	4.92	6.20	XP_008352163.1|1.9e-255|PREDICTED: TMV resistance protein N-like
MD15G1313900	1.96	3.38	5.63	XP_008359473.1|1.4e-208|PREDICTED: feruloyl CoA ortho-hydroxylase 1-like
MD00G1145300	−1.03	−5.12	1.42	XP_017184528.1|1.0e-249|PREDICTED: cyanogenic beta-glucosidase-like
MD17G1044100	−1.15	−5.25	−4.84	XP_017179832.1|2.1e-59|PREDICTED: uncharacterized protein LOC103404593 isoform X3
MD11G1030100	−1.73	−6.20	−6.19	XP_008339183.1|1.5e-216|PREDICTED: putative disease resistance RPP13-like protein 1
MD02G1226900	−1.78	−6.23	−4.22	XP_021814647.1|2.9e-308|protein ECERIFERUM 1-like
MD05G1060300	−2.07	−9.87	−1.58	XP_009362267.1|1.8e-209|PREDICTED: F-box protein SKIP19-like
MD00G1202500	−2.11	−2.09	−5.67	XP_009357592.1|1.1e-215|PREDICTED: putative pectate lyase 2
MD07G1097000	−2.19	−5.92	−5.75	XP_008343662.1|7.9e-139|PREDICTED: trihelix transcription factor ASIL2-like
MD09G1102100	−2.34	−5.91	−1.90	XP_009353363.1|1.7e-50|PREDICTED: uncharacterized protein LOC103944608
MD05G1257300	−2.71	−3.71	−6.98	XP_009353921.1|1.7e-201|PREDICTED: protein ROOT HAIR DEFECTIVE 3 homolog 2-like isoform X2
MD05G1362200	−2.71	−4.28	−5.27	XP_008363186.1|0.0e+00|PREDICTED: WEB family protein At1g12150-like
MD15G1246100	−2.95	−1.48	−5.38	XP_017192476.1|6.8e-55|PREDICTED: snakin-2-like
MD11G1170400	−3.60	−5.91	−4.31	XP_008346298.1|1.1e-103|PREDICTED: uncharacterized protein LOC103409262
MD13G1109500	−3.77	−5.75	−3.74	XP_008390113.1|3.9e-250|PREDICTED: BAHD acyltransferase At5g47980
MD13G1108500	−3.83	−3.70	−5.21	XP_008389779.1|2.1e-135|PREDICTED: small heat shock protein, chloroplastic-like
MD13G1146200	−3.92	−7.00	−3.63	XP_008390400.1|3.5e-128|PREDICTED: probable boron transporter 2 isoform X1
MD05G1008700	−4.18	−5.17	−4.16	XP_009366817.1|1.7e-141|PREDICTED: protein STAY-GREEN LIKE, chloroplastic-like
MD17G1020300	−4.27	−3.41	−6.57	XP_008379177.1|3.5e-75|PREDICTED: class I heat shock protein-like
MD07G1164500	−4.60	−5.58	−3.57	XP_009376050.1|2.2e-199|PREDICTED: WAT1-related protein At3g30340-like

Table 2 (continued)

Gene ID	$\log_2$ (R001/R000)	$\log_2$ (R003/R000)	$\log_2$ (R006/R000)	Search results
				Match|E value|gene annotation/function
MD01G1144200	−4.75	−4.11	−5.55	XP_009344315.1|8.7e-24|PREDICTED: 16.9 kDa class I heat shock protein 2-like
MD09G1237600	−4.77	−5.75	−3.74	XP_008381217.1|3.1e-103|PREDICTED: protein LIGHT-DEPENDENT SHORT HYPOCOTYLS 10-like
MD03G1127600	−5.03	−5.02	−2.34	XP_008357353.2|3.4e-160|PREDICTED: transcription factor FER-LIKE IRON DEFICIENCY-INDUCED TRANSCRIPTION FACTOR-like
MD12G1252500	−5.06	−2.72	−5.03	XP_008218371.1|4.0e-185|PREDICTED: GDSL esterase/lipase LTL1-like
MD10G1171200	−5.10	−4.35	−7.15	XP_008382664.1|6.4e-102|PREDICTED: 22.0 kDa class IV heat shock protein-like
MD07G1135800	−5.11	−5.10	−5.09	XP_008393387.1|5.1e-100|PREDICTED: uncharacterized protein LOC103455579
MD06G1065700	−5.18	−4.17	−4.16	XP_008373809.1|7.6e-126|PREDICTED: axial regulator YABBY 1-like
MD17G1226000	−5.19	−4.51	−6.39	XP_008342822.1|0.0e+00|PREDICTED: heat shock 70 kDa protein-like
MD01G1126000	−5.24	−5.23	−4.22	XP_008370768.2|3.9e-45|PREDICTED: uncharacterized protein LOC103434212 isoform X3
MD13G1106700	−5.26	−3.37	−2.07	XP_009359261.1|1.7e-93|PREDICTED: photosystem II core complex proteins psbY, chloroplastic
MD13G1104700	−5.27	−5.26	−3.44	XP_017192438.1|8.4e-307|PREDICTED: uncharacterized protein LOC103452050 isoform X2
MD05G1289300	−5.28	−3.43	−1.44	XP_008371583.1|2.6e-168|PREDICTED: chlorophyll a-b binding protein of LHCII type 1-like
MD07G1253800	−5.34	−2.69	−4.05	XP_008376419.1|3.2e-120|PREDICTED: 23.6 kDa heat shock protein, mitochondrial-like
MD05G1183400	−5.37	−4.03	−7.34	XP_008372421.1|8.9e-112|PREDICTED: 22.0 kDa class IV heat shock protein-like
MD16G1059700	−5.41	−4.39	−2.38	XP_008339790.1|7.4e-304|PREDICTED: cytochrome P450 78A5-like
MD06G1119300	−5.46	−6.44	−2.43	XP_008374120.1|0.0e+00|PREDICTED: cytochrome P450 78A9-like
MD13G1025600	−5.48	−3.32	−4.60	XP_008389221.1|3.7e-106|PREDICTED: chaperone protein DnaJ-like
MD05G1289200	−5.48	−3.81	−1.66	XP_008371581.1|1.7e-152|PREDICTED: chlorophyll a-b binding protein of LHCII type 1
MD11G1059800	−5.51	−4.49	−5.48	XP_008349637.1|1.1e-225|PREDICTED: isoleucine N-monooxygenase 1-like
MD03G1114700	−5.57	−5.51	−4.83	XP_008363505.1|1.6e-151|PREDICTED: fasciclin-like arabinogalactan protein 12
MD08G1249100	−5.60	−4.58	−5.57	XP_008357666.1|1.0e-112|PREDICTED: 22.0 kDa class IV heat shock protein-like
MD11G1169900	−5.60	−4.58	−2.99	XP_009344568.1|9.8e-75|PREDICTED: photosystem I subunit O-like isoform X2
MD10G1316300	−5.68	−5.08	−5.07	XP_008384041.2|3.6e-229|PREDICTED: beta-glucosidase 46-like isoform X3
MD03G1298400	−5.88	−3.55	−3.86	XP_009350185.1|1.2e-151|PREDICTED: uncharacterized protein LOC103941713
MD17G1140600	−6.18	−6.17	−4.16	XP_008342372.1|5.8e-174|PREDICTED: protodermal factor 1
MD13G1055700	−6.43	−5.42	−3.41	XP_008350880.1|2.2e-178|PREDICTED: DNA-3-methyladenine glycosylase-like
MD10G1265400	−6.49	−4.53	−1.82	XP_008356026.1|1.8e-152|PREDICTED: chlorophyll a-b binding protein of LHCII type 1

Table 2 (continued)

Gene ID	$\log_2$ (R001/R000)	$\log_2$ (R003/R000)	$\log_2$ (R006/R000)	Search results
				Match|E value|gene annotation/function
MD09G1128900	−6.60	−2.39	−1.60	XP_008229939.1|3.4e-30|PREDICTED: uncharacterized protein LOC103329269
MD17G1000100	−6.64	−3.34	−2.50	XP_009344942.2|4.4e-269|PREDICTED: premnaspirodiene oxygenase-like
MD03G1258300	−6.67	−2.85	−5.18	XP_008386414.1|1.8e-178|PREDICTED: heat stress transcription factor A-6b-like
MD12G1187100	−6.84	−5.83	−1.50	NP_001281295.1|1.7e-59|non-specific lipid-transfer protein precursor
MD02G1247700	−6.96	−6.94	−4.35	XP_008345531.1|0.0e+00|PREDICTED: trihelix transcription factor PTL-like
MD11G1278900	−7.47	−2.86	−4.87	XP_008386414.1|1.2e-217|PREDICTED: heat stress transcription factor A-6b-like
MD09G1066400	−7.78	−2.64	−2.23	XP_009365877.1|1.4e-192|PREDICTED: protein RIK-like isoform X1
MD03G1218900	−7.79	−5.77	−2.76	XP_008366442.1|3.9e-153|PREDICTED: chlorophyll a-b binding protein 13, chloroplastic
MD04G1174000	−7.87	−5.85	−4.03	XP_008370253.1|1.0e-65|PREDICTED: non-specific lipid-transfer protein 3-like
MD10G1265300	−7.87	−3.24	−1.13	XP_008371583.1|3.3e-152|PREDICTED: chlorophyll a-b binding protein of LHCII type 1-like
MD16G1070500	−7.99	−7.97	−7.96	XP_008339883.1|1.4e-247|PREDICTED: uncharacterized protein LOC103402884
MD03G1114600	−8.83	−9.81	−4.10	XP_008344850.1|1.6e-78|PREDICTED: fasciclin-like arabinogalactan protein 12

carbonic anhydrase, and cyanate lyase are all involved in nitrate–nitrogen absorption and metabolism (Ye et al. 2019; Fig. 6a). Figure 6b shows the heatmap of 43 genes involved in N absorption and metabolism. Our data suggest that tea crabapple may respond to MSAS by regulating the expression levels of N metabolism-related genes.

Phosphate transporter, purple acid phosphatase, acid phosphatase, 6-phosphogluconate dehydrogenase, triose phosphate/phosphate translocator, patellin-5, phospholipase A1-II, 4-hydroxy-3-methylbut-2-en-1-yl diphosphate synthase, and phosphatidylinositol/phosphatidylcholine transfer protein SFH are all involved in P absorption and metabolism (Ye et al. 2019), while K channel, K transporter, cation/H⁺ antiporter, and CBL-interacting protein kinase play a key role in K absorption and metabolism (Xu et al. 2019). The expression levels of genes involved in P and K absorption and metabolism are shown in Tables 4 and 5, respectively. As evident, the expression levels of most genes were downregulated. We believe that these gene expression changes play a pivotal role making tea crabapple tolerant to MSAS.

qRT-PCR Verification

qRT-PCR was performed to validate the expression levels of six genes: two TF-coding genes (MD01G1090900, MD03G1258300), two nitrate absorption and metabolism-related genes (MD03G1165000, MD15G1173800), one P absorption and metabolism-related gene (MD14G1118000), and one K absorption and metabolism-related gene (MD04G1124400). As evident from Fig. 7, the up- or downregulation of these genes in response to MSAS was consistent between qRT-PCR and RNA-seq; however, some genes (MD03G1258300, MD04G1124400, MD15G1173800) showed a slightly inconsistent behavior, which could be due to differences in sample processing and detection methods.

Discussion

The Yellow River Delta is an important grain production base in China. In recent years, the presence of the apple industry has become predominant in this region. However, considering its geographical location and natural conditions, soil salinization–alkalization is a serious concern, which has markedly hindered apple cultivation and yield. MSAS is a type of abiotic stress that severely restricts plant growth (Jia et al. 2019) and damages the photosynthetic system; moreover, under severe stress conditions, even plant death can occur (Abbasi et al. 2015). Therefore, for breeding novel salt-tolerant crop varieties, it is pivotal to study the response of apple trees to MSAS. In this study, we performed RNA-seq to measure gene expression levels in the roots of tea

Table 3 Genes encoding transcription factors

Transcription factor family	Total number of transcription factors	Number of differentially expressed transcription factors			
		Total (%)	R001/R000	R003/R000	R006/R000
AP2-EREBP	218	69 (31.65)	38	25	39
MYB	329	62 (18.84)	42	22	45
bHLH	190	44 (26.16)	28	28	22
NAC	173	34 (19.65)	13	6	23
WRKY	120	29 (24.17)	15	7	24
HSF	38	15 (39.47)	11	9	13
C2C2-Dof	50	14 (28.00)	9	7	9
C3H	107	13 (12.15)	9	6	10
GRAS	90	13 (14.44)	8	6	6
LOB	70	12 (17.14)	8	6	10
G2-like	66	11 (16.67)	7	2	9
C2H2	84	10 (11.90)	6	4	9
Trihelix	57	9 (15.79)	7	4	7
C2C2-CO-like	17	9 (52.94)	7	5	6
TCP	36	9 (25.00)	6	2	6
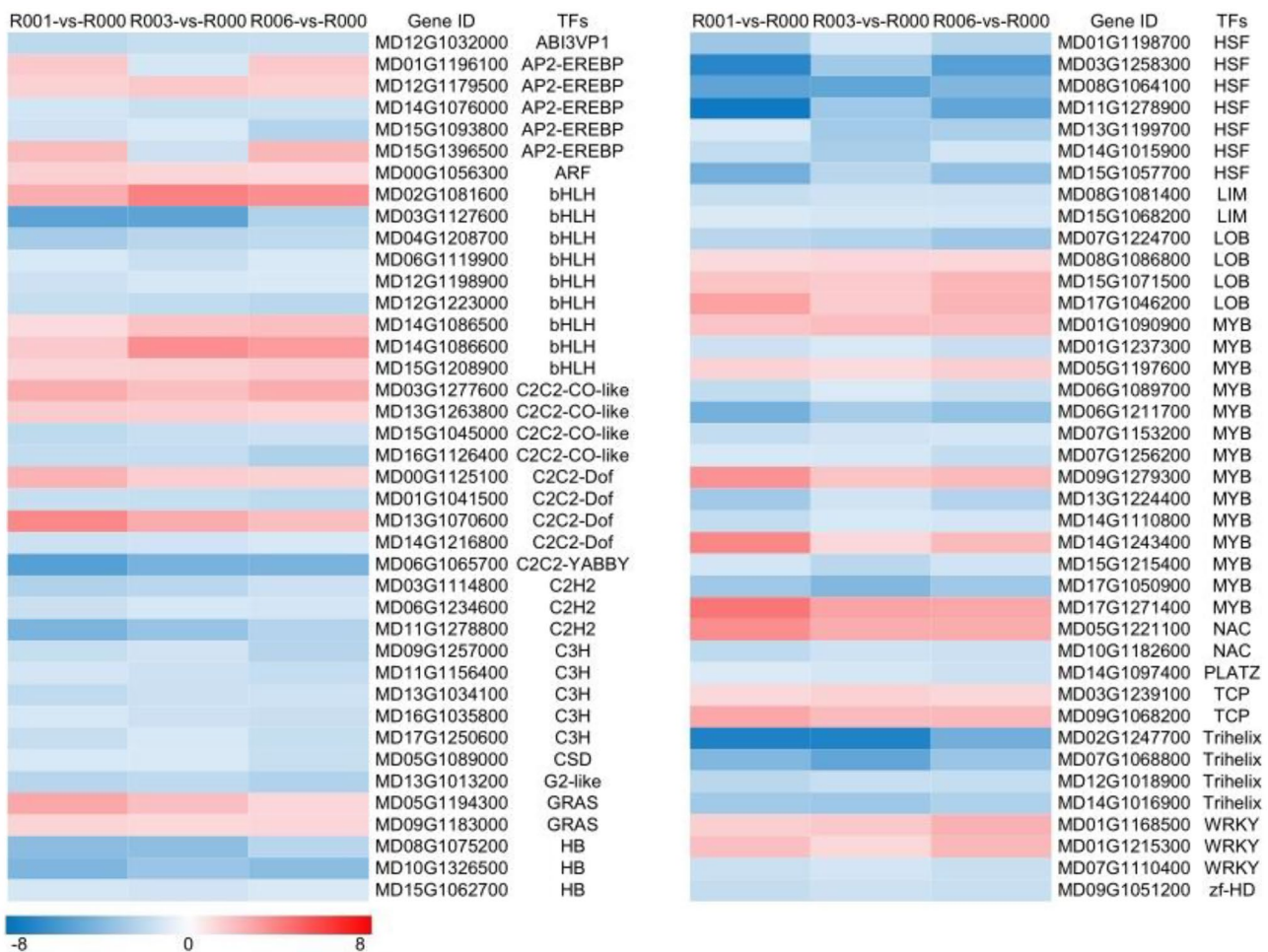
Fig. 4 Heatmap showing differentially expressed transcription factor-coding genes in 1022 common DEGs (yellow part in Fig. 1B) in tea crabapple roots upon mixed saline–alkali stress exposure. Red and blue indicate genes with up- and downregulated expression levels, respectively
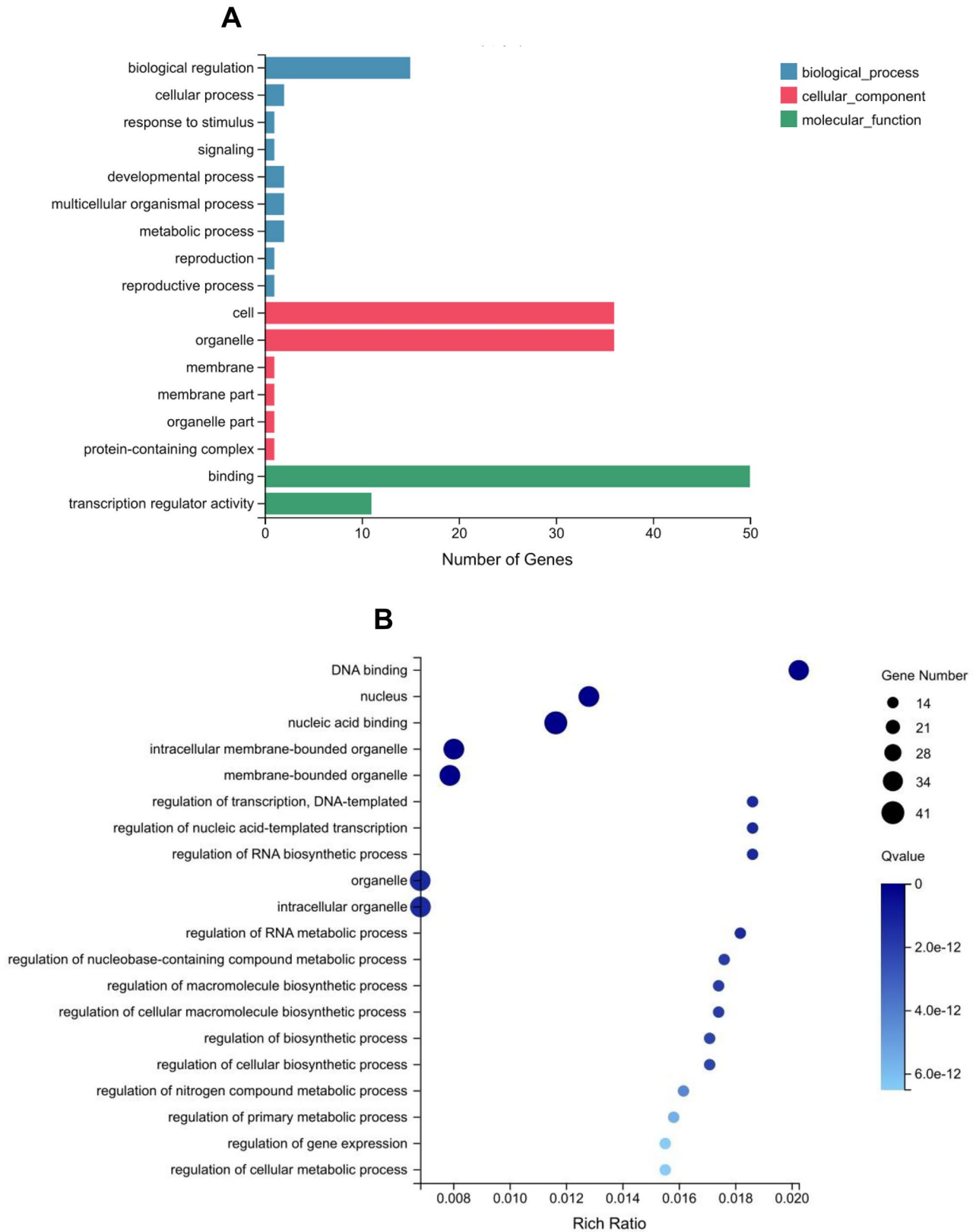
Fig. 5 Gene ontology analysis of differentially expressed transcription factor-coding genes in 1022 common DEGs (yellow part in Fig. 1B). **A** Classification. **B** Enrichment analysis
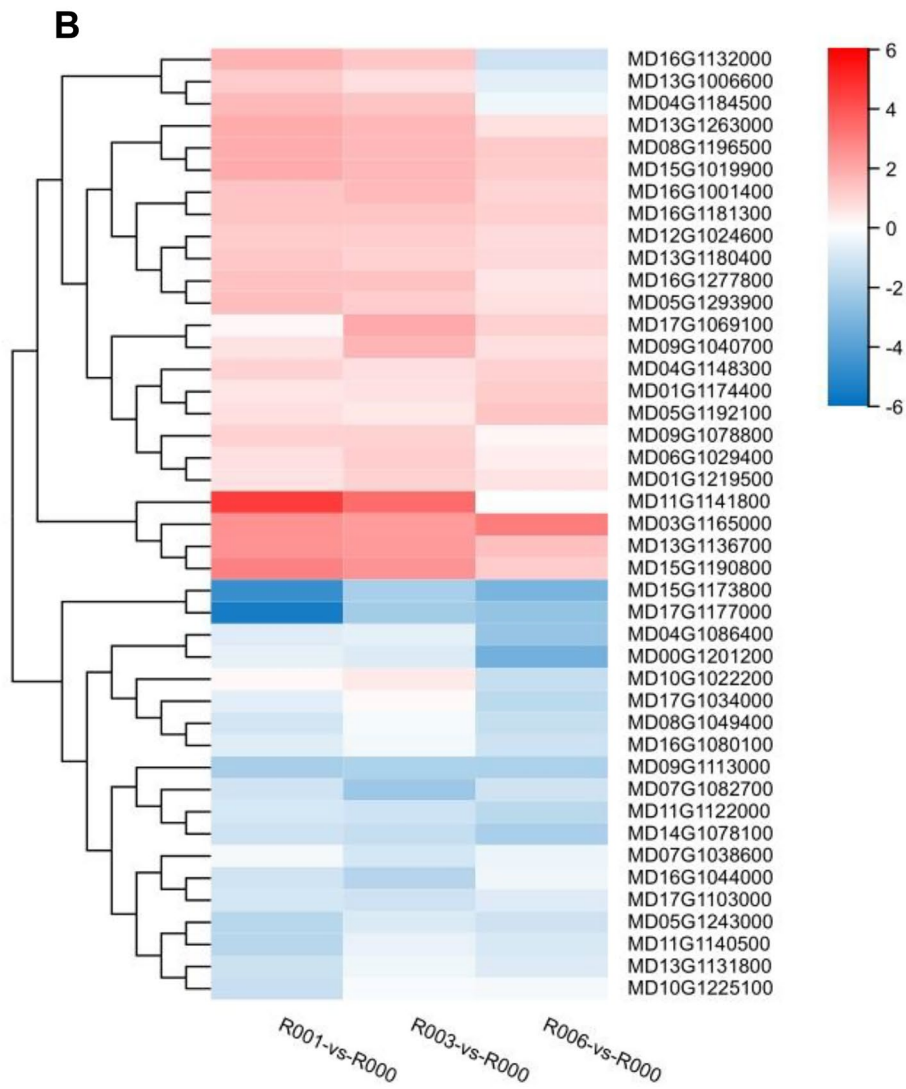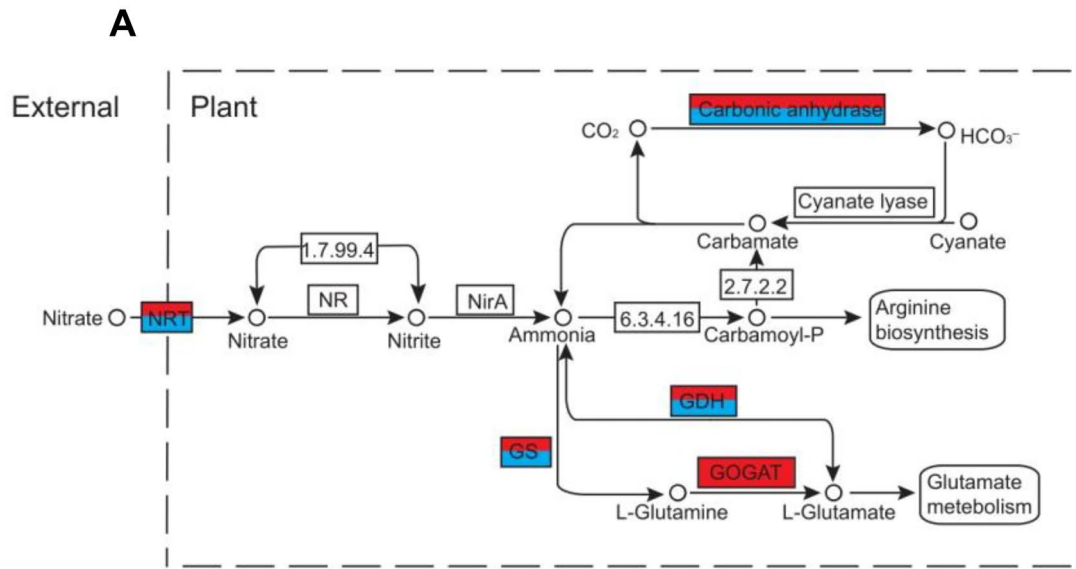
A

B

◄**Fig. 6** Genes involved in nitrate uptake and metabolism in tea crabapple roots that responded to MSAS in at least one comparison group (all genes in Fig. 1B). **A** Nitrate absorption and metabolism pathway upon MSAS exposure. Red: upregulated in comparison with the control. Blue: downregulated in comparison with the control. **B** Heatmap of the expression of genes involved in nitrate absorption and metabolism upon MSAS exposure. NRT (MD00G1201200, MD04G1086400, MD04G1148300, MD04G1184500, MD05G1192100, MD05G1293900, MD06G1029400, MD07G1038600, MD07G1082700, MD09G1040700, MD09G1113000, MD11G1122000, MD11G1141800, MD13G1131800, MD13G1136700, MD15G1019900, MD15G1173800, MD15G1190800, MD16G1044000, MD16G1080100, MD16G1132000, MD16G1277800, MD17G1103000); GS (MD05G1243000, MD08G1049400, MD09G1078800, MD10G1225 100, MD13G1006600, MD13G1180400, MD13G1263000, MD16G100 1400, MD16G1181300, MD17G1069100); GOGAT (MD01G1219500); GDH (MD01G1174400, MD17G1177000); carbonic anhydrase (MD03G 1165000, MD08G1196500, MD10G1022200, MD11G1140500, MD12G 1024600, MD14G1078100, MD17G1034000)

crabapple seedlings exposed to MSAS, which led to the identification of 2931, 2335, and 3746 DEGs (up- or downregulated) at R001, R003, and R006 of MSAS exposure, respectively. The number of DEGs and up- and downregulated genes all reached their lowest point in 3d, indicating that the response to MSAS appeared turning point in 3d. At each timepoint, the number of downregulated genes was higher than that of upregulated genes, which is similar to the results obtained upon subjecting wild soybean roots to $NaHCO_3$ stress (Ge et al. 2010), but different from those obtained upon subjecting *Cynanchum auriculatum* leaves to saline stress (Zhang et al. 2020). These discrepancies could be due to differences is plant stress responses to different ions and high pH conditions during MSAS; moreover, plants tend to experience more serious damage when exposed to a combination of stresses than under a single stress condition (Ge et al. 2010).

In the three comparison groups, 1022 overlapping DEGs were identified. GO enrichment analyses of these DEGs showed that the biological processes category was the most abundant, followed by the cellular components and molecular function categories. "Binding" and "catalytic activity" were the most abundant subcategories across all three categories. Consistent with this result, "binding" and "catalytic activity" were the most abundant subcategories even when *Vitis vinifera* was exposed to salt stress (Das and Majumder 2019). Such results collectively indicate that these two subcategories are the main processes used by plants to withstand MSAS. In the cellular components category, "membrane" and "membrane part" were the most abundant subcategories, and in the biological processes category, "metabolic process" and "cellular process" were the most abundant. On exposing *C. auriculatum* leaves to saline stress, Zhang et al. (2020) reported that the most enriched subcategories in the cellular components and biological processes categories were "membrane part" and "cellular process" respectively, and when sugar sorghum was subjected

to saline–alkali stress, Dai et al. (2016) found that the most abundant subcategories in the cellular components and biological processes categories were "cell" and "metabolic process" respectively. Therefore, we concluded that the "binding," "catalytic activity," "membrane," "membrane part," "metabolic process," and "cellular process" subcategories play a role in the response of tea crabapple roots to MSAS.

KEGG pathway enrichment analysis revealed that the metabolism category was the most abundant, with "global and overview maps" being the most abundant subcategory within this category. In addition, "folding, sorting, and degradation"; "signal transduction"; "environmental adaptation"; and "transport and catabolism" were the most abundant subcategories in the genetic information processing, environmental information processing, organismal systems, and cellular processes categories, respectively. Similarly, Das and Majumder (2019) reported that on exposing *V. vinifera* leaves to salt stress, the carbohydrate metabolism, signal transduction, energy metabolism, amino acid metabolism, biosynthesis of secondary metabolite, and lipid metabolism pathways possessed the largest number of transcripts.

On exposing two types of apple rootstocks (*M. halliana* and *M. robusta*) to short-term salt stress, Zhu et al. (2019) observed a decrease in chlorophyll (including chlorophyll a and b) content, net photosynthetic rate, and stomatal conductance. Herein, when tea crabapple seedlings were subjected to MSAS, the expression levels of five chlorophyll a/b binding protein encoding genes (MD03G1218900, MD05G1289200, MD05G1289300, MD10G1265300, and MD10G1265400) were significantly reduced (Table 2). Although their expression was significantly inhibited upon MSAS exposure, their expression levels in the roots of tea crabapple seedlings were very low (Table S10).

Heat shock proteins (HSPs) are significantly expressed in plants in response to environmental stresses. They play a key role in helping plants recover from heat stress-induced injury and improve heat resistance (Hu et al. 2009). Furthermore, they facilitate the stabilization of chromatin structures, proteins, and membranes and also promote protein repair during or after stress exposure by refolding (Wang et al. 2014). Based on molecular weight, the HSP family can be classified into five groups: small HSPs, HSP60s, HSP70s, HSP90s, and HSP100s (Jiang et al. 2009). In $NaHCO_3$-stressed *Tamarix hispida* roots, Wang et al. (2014) found that the expression levels of some HSPs were either up- or downregulated. We found that the expression levels of eight HSPs (MD01G1144200, MD05G1183400, MD07G1253800, MD08G1249100, MD10G1171200, MD13G1108500, MD17G1020300, and MD17G1226000) were downregulated upon MSAS exposure (Table 2), validating that plant HSPs play a role in MSAS response. However, it is notable that HSP expression levels vary depending on several factors, such as stress severity and plant species.

Table 4 Differentially expressed genes involved in phosphorous absorption and metabolism

| Gene ID	log$_2$ (R001/R000)	Q value	log$_2$ (R003/R000)	Q value	log$_2$ (R006/R000)	Q value	Gene function annotation
MD00G1081300	0.60	9.22E-07	0.02	0.314695	1.06	8.81E-21	Phosphate transporter PHO1 homolog 3-like
MD16G1222100	0.78	0	1.12	0	0.57	2.34E-214	Phosphate transporter PHO1-like isoform X2
MD01G1214700	1.88	4.92E-175	1.84	7.79E-166	0.30	0.000450	Inorganic phosphate transporter 1–11-like
MD10G1275200	0.37	0.025363	1.31	1.41E-15	0.25	0.077164	Sodium-dependent phosphate transporter 1-like
MD07G1284400	1.46	9.19E-67	1.29	7.94E-49	− 0.64	1.52E-07	Inorganic phosphate transporter 1–11-like
MD17G1052300	− 0.79	2.41E-24	− 0.71	3.16E-20	− 1.12	5.59E-42	Phosphate transporter PHO1 homolog 9
MD16G1102200	− 0.65	7.76E-07	− 0.15	0.111353	− 1.13	2.70E-15	Inorganic phosphate transporter 2–1, chloroplastic-like
MD16G1217400	0.59	0.018012	1.00	0.000110	− 0.70	0.020294	Probable inorganic phosphate transporter 1–7
MD07G1046300	− 1.02	3.32E-101	− 0.58	7.49E-39	− 1.75	3.64E-226	Probable inorganic phosphate transporter 1–5
MD14G1118000	1.01	4.19E-191	1.12	4.50E-241	0.74	2.61E-93	6-Phosphogluconate dehydrogenase, decarboxylating 2, chloroplastic isoform X1
MD14G1117900	1.05	0	1.17	0	0.77	3.94E-194	6-Phosphogluconate dehydrogenase, decarboxylating 2, chloroplastic
MD05G1310100	− 2.28	2.71E-11	− 1.73	3.79E-08	− 1.67	5.31E-08	Triose phosphate/phosphate translocator, chloroplastic isoform X1
MD05G1265900	− 0.59	2.43E-58	− 1.04	1.65E-151	− 1.24	5.71E-200	Patellin-4-like isoform X2
MD11G1004600	− 0.53	0.041226	− 0.64	0.027113	− 1.28	0.000173	Phospholipase A1-IIdelta
MD05G1277700	1.65	2.50E-116	− 0.01	0.315010	1.43	1.43E-80	Phospholipase A1-Igamma1, chloroplastic-like
MD05G1278100	1.35	3.37E-09	0.32	0.121814	1.21	2.00E-07	Phospholipase A1-Igamma1, chloroplastic-like
MD05G1278200	1.34	6.38E-165	0.44	1.00E-13	1.09	9.60E-100	Phospholipase A1-Igamma1, chloroplastic-like
MD10G1070400	− 1.13	3.67E-36	− 0.85	1.38E-22	− 1.76	3.26E-68	Phosphatidylinositol/ phosphatidylcholine transfer protein SFH3-like
MD00G1060800	− 2.78	3.12E-57	− 2.55	5.87E-52	− 2.80	3.48E-57	Acid phosphatase 1-like
MD14G1240300	− 1.29	1.98E-60	− 0.62	1.75E-18	− 1.16	5.71E-51	Purple acid phosphatase 17-like
MD12G1023400	− 0.59	1.81E-08	− 0.29	0.002842	− 1.03	9.55E-20	Probable purple acid phosphatase 20
MD04G1009800	0.85	8.15E-13	0.89	7.14E-14	1.26	8.39E-30	Purple acid phosphatase 15-like
MD16G1013600	− 0.44	0.007039	− 1.00	3.14E-07	− 1.09	2.27E-08	Purple acid phosphatase 3
MD01G1098300	− 1.29	4.63E-122	− 1.06	1.33E-89	− 1.26	2.08E-117	Probable inactive purple acid phosphatase 29
MD07G1029700	1.00	2.63E-06	0.61	0.006314	0.34	0.062523	Probable inactive purple acid phosphatase 27
MD09G1201200	− 1.46	2.06E-152	− 0.76	1.38E-52	− 1.22	1.05E-114	Acid phosphatase 1-like
MD09G1200900	− 1.01	3.14E-174	− 0.47	5.11E-46	− 0.88	8.53E-138	Acid phosphatase 1-like
MD14G1080200	− 0.85	2.57E-06	− 0.50	0.002753	− 1.10	6.87E-09	Probable inactive purple acid phosphatase 16
MD15G1020000	− 1.31	1.99E-108	− 0.68	1.37E-36	− 1.23	1.29E-97	Purple acid phosphatase 2

Table 4 (continued)

Gene ID	log$_2$ (R001/R000)	Q value	log$_2$ (R003/R000)	Q value	log$_2$ (R006/R000)	Q value	Gene function annotation
MD12G1023300	− 0.24	1.33E-09	− 0.53	2.79E-36	− 1.18	2.67E-142	Purple acid phosphatase 22
MD07G1161500	0.38	0.087241	1.07	6.13E-05	2.02	5.15E-19	Soluble inorganic pyrophosphatase 1
MD15G1061100	0.77	1.02E-46	1.15	2.09E-115	0.54	2.18E-21	Inorganic pyrophosphatase 2-like

Table 5 Differentially expressed genes involved in potassium absorption and metabolism

Gene ID	log$_2$ (R001/R000)	Q value	log$_2$ (R003/R000)	Q value	log$_2$ (R006/R000)	Q value	Gene function annotation
MD15G1178200	1.51	2.09E-39	− 0.35	0.019148	2.21	3.12E-104	Potassium channel AKT1-like
MD10G1230200	0.35	0.005379	0.68	9.70E-08	1.08	7.90E-20	Potassium transporter 10-like
MD09G1267300	1.46	0	1.37	7.55E-302	0.81	3.08E-88	Potassium channel SKOR isoform X4
MD08G1236000	− 1.27	4.14E-19	− 0.63	7.79E-07	− 1.00	1.72E-13	Potassium channel
MD10G1204500	2.48	4.39E-08	1.89	0.000162	− 1.06	0.078318	Probable potassium transporter 13
MD07G1232700	− 0.39	3.34E-16	− 0.37	1.51E-14	− 1.11	4.34E-94	Potassium transporter 2-like isoform X2
MD11G1302600	− 1.11	7.07E-31	− 0.12	0.068324	− 1.15	2.48E-32	Potassium transporter 5
MD11G1200700	− 1.16	2.09E-09	− 1.03	8.41E-08	− 1.34	2.22E-11	Two-pore potassium channel 1-like
MD01G1165900	− 0.98	2.46E-24	− 1.01	3.24E-25	− 1.63	1.08E-51	Potassium transporter 2-like
MD03G1183700	− 2.06	1.34E-11	− 2.66	5.95E-15	− 1.84	3.35E-10	Two-pore potassium channel 1-like isoform X1
MD10G1230100	− 1.05	0.029174	− 5.57	5.40E-06	− 1.96	0.001505	Potassium transporter 10-like
MD04G1124700	− 1.98	6.53E-52	− 1.91	4.69E-49	− 1.10	1.91E-22	Cation/H(+) antiporter 20-like
MD07G1228400	− 1.45	0.033141	− 4.75	0.000638	− 1.42	0.031055	Cation/H(+) antiporter 15-like
MD04G1124400	− 2.08	0	− 0.87	3.33E-158	− 1.63	0	Cation/H(+) antiporter 20-like
MD04G1124500	− 0.51	0.101749	− 0.21	0.246512	− 5.98	1.03E-07	Cation/H(+) antiporter 20-like
MD13G1203400	1.41	1.17E-107	0.57	6.87E-14	0.82	2.07E-30	CBL-interacting serine/threonine-protein kinase 4-like
MD15G1153500	− 1.04	0	− 0.13	1.06E-14	− 0.91	0	CBL-interacting serine/threonine-protein kinase 6-like
MD00G1143400	− 0.59	6.73E-25	− 0.05	0.160653	− 1.04	9.84E-63	CBL-interacting serine/threonine-protein kinase 5-like
MD02G1008400	− 1.43	5.97E-40	− 0.61	1.55E-10	− 1.34	3.57E-36	CBL-interacting serine/threonine-protein kinase 6-like
MD13G1139700	− 0.67	1.24E-38	− 0.59	5.59E-31	− 1.20	1.46E-100	CBL-interacting serine/threonine-protein kinase 1-like
MD07G1157500	0.80	9.06E-35	0.60	9.05E-19	1.01	5.79E-58	CBL-interacting serine/threonine-protein kinase 9
MD12G1011500	− 0.98	0.012487	− 1.96	0.000115	− 2.47	6.57E-06	Cation/calcium exchanger 1

Fig. 7 Quantitative real-time PCR (qRT-PCR) to validate the expression levels of six genes that responded to mixed saline–alkali stress. Transcription factor-coding genes: MD01G1090900, MD03G1258300; nitrate absorption and metabolism-related genes: MD03G1165000, MD15G1173800; phosphorus absorption and metabolism-related genes: MD14G1118000; and potassium absorption and metabolism-related gene: MD04G1124400
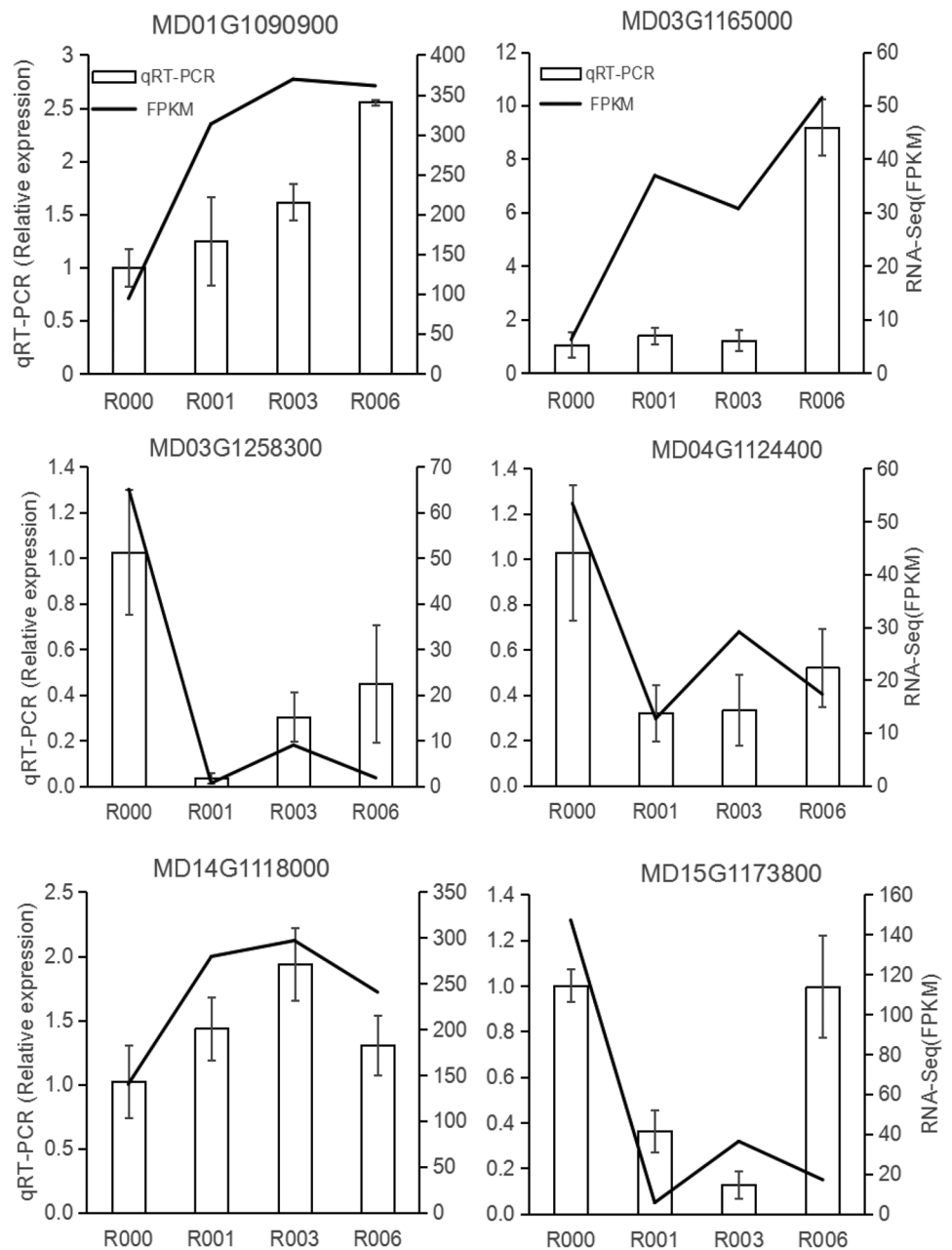
CYP450 is a large family of enzyme proteins in microorganisms, animals, and plants. In plants, they are involved in the biosynthesis of auxins, gibberellins, cytokinins, and other endogenous hormones, as well as in that of many secondary metabolites (Xu et al. 2015). Khanom et al. (2019) found that the expression level of *PgCYP736A12*, which is involved in herbicide metabolism, in ginseng (*Panax ginseng* Meyer) was upregulated after NaCl treatment. The number of cells in a CYP78A5 mutant decreased, while that of cells in plants overexpressing CYP78A5 or CYP78A9 increased, suggesting their involvement in organ size regulation via cell proliferation (Anastasiou et al. 2007; Ito and Meyerowitz 2000). Furthermore, CYP78A9 has been reported to play

an important role in regulating the fruit size of sweet cherry (*Prunus avium* L.) (Qi et al. 2017). In the present study, the expression level of one CYP736A12-like protein-coding gene (MD11G1219700) was upregulated, while that of one CYP78A5-like protein-coding gene (MD16G1059700) and one CYP78A9-like protein-coding gene (MD06G1119300) was downregulated. These findings suggested that CYP450s play a role in the response of tea crabapple to MSAS.

Herein, we observed that some disease-resistant proteins (MD11G1030100), non-specific lipid-transfer proteins (MD04G1174000 and MD12G1187100), pectate lyase (MD00G1202500), and beta-glucosidases (MD10G1316300, MD00G1145300, and MD14G1080000) significantly responded

to MSAS. Beta-glucosidase is involved in cell wall hydrolysis and plays a role in many functions, such as defense, plant hormone regulation, and oligosaccharide catabolism (Jin et al. 2008). Its activity is optimal at pH 5.0, indicating that the expression level of the gene encoding beta-glucosidase may be downregulated under high pH conditions (Opassiri et al. 2003). This suggests that the aforementioned genes have a role not only in disease resistance, lipid transport, and cell wall hydrolysis but also in the response of tea crabapple to MSAS.

Salt stress has a negative regulatory effect on the activities of N absorption and assimilation-related enzymes and coding genes in many plants (Miura 2013). In the present study, upon MSAS exposure, the expression levels of several genes involved in nitrate absorption and assimilation, such as NRT, GS, GOGAT, GDH, and carbonic anhydrase, were up- or downregulated in tea crabapple roots. Demiral (2017) investigated the effects of salt stress on N and P concentrations in the leaves and roots of two strawberry cultivars and found that cultivar and sampling time significantly affected their concentrations. In this study, the expression levels of some P absorption and metabolism-related genes were upregulated, while those of some were downregulated. In addition, the expression levels of most K absorption and metabolism-related genes were downregulated upon exposure to MSAS. Jia et al. (2019) subjected *M. halliana* to salt stress, alkali stress, and MSAS and found that in comparison with salt stress and MSAS treatments, *M. halliana* accumulated more Na^+ in roots and less K^+ in leaves under alkali stress. Furthermore, Shi and Wang (2005) reported that under MSAS, Na^+ content increased while K^+ content decreased with an increase in salinity and pH in *Aneurolepidium chinense* (Trin.) Kitag. Collectively, these data suggest that tea crabapple has evolved a comprehensive regulatory mechanism to cope with MSAS.

TFs play a key role in regulating plant responses to various internal and external stimuli (Wang et al. 2014). We found that genes encoding many TFs (such as trihelix TFs, HSFs, and Fer-like iron deficiency-induced TFs) significantly responded to MSAS (Table 2), indicating their potential role in conferring tolerance to tea crabapple against MSAS. AP2-EREBPs responded the most to MSAS (Table 3), and MYBs were the most expressed in the three comparison groups (Fig. 4). In plants, the MYB family is one of the largest families of TFs (Wu et al. 2017). In this study, 62 MYB TFs were induced in response to MSAS (Table 3), and 14 genes were differentially expressed (five were upregulated and nine were downregulated) in the three comparison groups (Fig. 4). Li et al. (2020) performed genome-wide characterization of the *MYB* family in sunflower and investigated expression patterns of 55 selected *HaMYB* genes for different stresses. They found that the expression levels of nine of the 55 *HaMYB* genes were downregulated under simulated drought and salt stress; furthermore, the expression levels of *HaMYB15.3*, *HaMYB15.14*, *HaMYB15.10*, and *HaMYB102.5* were upregulated in roots but downregulated in leaves. Besides, another study reported MYB111 to be a positive regulator in salt stress response; MYB111 deficiency was observed to significantly decrease salt tolerance in *Arabidopsis* (Li et al. 2019). In general, gene expression profiles under different stress conditions are often different, implying that abiotic stress signaling pathways are complex (Xu et al. 2020; Li et al. 2020).

On MSAS exposure, the expression levels of seven *HSFs* in tea crabapple roots were found to be downregulated in the three comparison groups (Fig. 4). Heat shock response involves two important members: HSPs and HSFs. Chandel et al. (2013) studied the differential expression of *HSPs* and *HSFs* in rice exposed to different heat stress levels, and they found higher expression levels for most *HSP* and *HSF* genes, which contributed to greater thermal stress tolerance. HSFs reportedly control the response of plants to different environmental stresses (biotic plus abiotic) by regulating the expression of HSP-coding genes.

Nine members of the bHLH TF family were differentially expressed in the three comparison groups, of which five genes (MD02G1081600, MD03G1127600, MD06G1119900, MD14G1086500, and MD15G1208900) were found to belong to MYC2 and thus participate in the mitogen-activated protein kinase and jasmonic acid signal transduction pathways (Liu et al. 2019). MD05G1194300 and MD09G1183000 represent aspartic acid–glutamic acid–leucine–leucine–alanine proteins (DELLAs, a group of proteins belonging to the GRAS family), and MD12G1198900 is a phytochrome-interacting factor (also belonging to the bHLH TF family); they are involved in the gibberellin signal transduction pathway (Vera-Sirera et al. 2016). MD00G1056300 is an auxin response factor, playing a role in auxin signal transduction pathways. MD13G1013200 is a type-B authentic response regulator with a GARP-like DNA binding domain at the C-termini; it is involved in the cytokinin signal transduction pathway and regulates plant growth and development (Xie et al. 2018). Herein, signal transduction-related genes encoding various hormones (e.g., auxin, gibberellin, and jasmonic acid) were found to be involved in plant stress response (Liu et al. 2019; Vera-Sirera et al. 2016).

Other types of TFs, such as AP2-EREBP, C3H, C2C2-Dof, C2C2-CO-like, and WRKY, also responded to MSAS exposure. In model plants, they participate in various processes, playing key roles in abiotic and biological stresses (Singh et al. 2002). In this study, many different members of TF families were induced in response to MSAS, indicating that a complex transcriptional regulatory network is used by tea crabapple to withstand MSAS. We believe that elucidating the function of such TFs should facilitate comprehensive investigations of transcriptional regulatory mechanisms used by tea crabapple to adapt to environmental stresses.

Declarations

Conflict of Interest The authors declare no competing interests.

References

Abbasi GH, Akhtar J, Ahmad R, Jamil M, Anwar-ul-Haq M, Ali S, Ijaz M (2015) Potassium application mitigates salt stress differentially at different growth stages in tolerant and sensitive maize hybrids. Plant Growth Regul 76:111–125. https://doi.org/10.1007/s10725-015-0050-1

Anastasiou E, Kenz S, Gerstung M, MacLean D, Timmer J, Fleck C, Lenhard M (2007) Control of plant organ size by KLUH/CYP78A5-dependent intercellular signaling. Dev Cell 13:843–856. https://doi.org/10.1016/j.devcel.2007.10.001

Chandel G, Dubey M, Meena R (2013) Differential expression of heat shock proteins and heat stress transcription factor genes in rice exposed to different levels of heat stress. J Plant Biochem Biotechnol 22:277–285. https://doi.org/10.1007/s13562-012-0156-8

Dai L, Yin K, Zhang Y, Yu C, Li M, Du J (2016) Screening and analysis of soda saline-alkali stress induced up- regulated genes in sugar sorghum. Maydica 61:9

Das P, Majumder AL (2019) Transcriptome analysis of grapevine under salinity and identification of key genes responsible for salt tolerance. Funct Integr Genomics 19:61–73. https://doi.org/10.1007/s10142-018-0628-6

Demïral M (2017) Effect of salt stress on concentration of nitrogen and phosphorus in root and leaf of strawberry plant. EJSS 6:357–364. https://doi.org/10.18393/ejss.319198

FAOSTAT (2020) http://www.fao.org/faostat/en/#data/QC. Accessed 5 Nov 2020

Ge Y, Li Y, Zhu Y, Bai X, Lv DK, Guo D, Ji W, Cai H (2010) Global transcriptome profiling of wild soybean (*Glycine soja*) roots under NaHCO₃ treatment. BMC Plant Biol 10:153. https://doi.org/10.1186/1471-2229-10-153

Hu W, Hu G, Han B (2009) Genome-wide survey and expression profiling of heat shock proteins and heat shock factors revealed overlapped and stress specific response under abiotic stresses in rice. Plant Sci 176:583–590. https://doi.org/10.1016/j.plantsci.2009.01.016

Ito T, Meyerowitz EM (2000) Overexpression of a gene encoding a cytochrome P450, *CYP78A9*, induces large and seedless fruit in *Arabidopsis*. Plant Cell 12:1541–1550. https://doi.org/10.1105/tpc.12.9.1541

Jia X, Wang H, Svetla S, Zhu Y, Hu Y, Cheng L, Zhao T, Wang Y (2019) Comparative physiological responses and adaptive strategies of apple *Malus halliana* to salt, alkali and saline-alkali stress. Sci Hortic 245:154–162. https://doi.org/10.1016/j.scienta.2018.10.017

Jiang C, Xu J, Zhang H, Zhang X, Shi J, Li M, Ming F (2009) A cytosolic class I small heat shock protein, RcHSP17. 8, of Rosa chinensis confers resistance to a variety of stresses to *Escherichia coli*, yeast and *Arabidopsis thaliana*. Plant Cell Environ 32:1046–1059. https://doi.org/10.1111/j.1365-3040.2009.01987.x

Jin H, Kim HR, Plaha P, Liu SK, Park JY, Piao YZ, Yang ZH, Jiang GB, Kwak SS, An G, Son M, Jin YH, Sohn JH, Lim YP (2008) Expression profiling of the genes induced by Na₂CO₃ and NaCl stresses in leaves and roots of *Leymus chinensis*. Plant Sci 175:784–792. https://doi.org/10.1016/j.plantsci.2008.07.016

Jung S, Lee T, Cheng CH, Buble K, Zheng P, Yu J, Humann J, Ficklin SP, Gasic K, Scott K, Frank M, Ru S, Hough H, Evans K, Peace C, Olmstead M, DeVetter LW, McFerson J, Coe M, Wegrzyn JL, Staton ME, Abbott AG, Main D (2019) 15 years of GDR: new data and functionality in the Genome Database for Rosaceae. Nucleic Acids Res 47:D1137–D1145. https://doi.org/10.1093/nar/gky1000

Khan SA, Li MZ, Wang SM, Yin HJ (2018) Revisiting the role of plant transcription factors in the battle against abiotic stress. Int J Mol Sci 19:1634. https://doi.org/10.3390/ijms19061634

Khanom S, Jang J, Lee OR (2019) Overexpression of ginseng cytochrome P450 *CYP736A12* alters plant growth and confers phenylurea herbicide tolerance in *Arabidopsis*. J Ginseng Res 43:645–653. https://doi.org/10.1016/j.jgr.2019.04.005

Langmead B, Trapnell C, Pop M, Salzberg SL (2009) Ultrafast and memory-efficient alignment of short DNA sequences to the human genome. Genome Biol 10:R25. https://doi.org/10.1186/gb-2009-10-3-r25

Li B, Fan R, Guo S, Wang P, Zhu X, Fan Y, Chen Y, He K, Kumar A, Shi J (2019) The *Arabidopsis* MYB transcription factor, MYB111 modulates salt responses by regulating flavonoid biosynthesis. Environ Exp Bot 166:103807. https://doi.org/10.1016/j.envexpbot.2019.103807

Li J, Liu H, Yang C, Wang J, Yan G, Si P, Bai Q, Lu Z, Zhou W, Xu L (2020) Genome-wide identification of MYB genes and expression analysis under different biotic and abiotic stresses in *Helianthus annuus* L. Ind Crops Prod 143:111924. https://doi.org/10.1016/j.indcrop.2019.111924

Liu Y, Du M, Deng L, Shen J, Fang M, Chen Q, Lu Y, Wang Q, Li C, Zhai Q (2019) MYC2 Regulates the termination of jasmonate signaling via an autoregulatory negative feedback loop. Plant Cell 31:106–127. https://doi.org/10.1105/tpc.18.00405

Miura K (2013) Nitrogen and phosphorus nutrition under salinity stress. In: Ahmad P, Azooz M, Prasad M (ed) Ecophysiology and responses of plants under salt stress. Springer, New York, pp 425–441. https://doi.org/10.1007/978-1-4614-4747-4_16

Opassiri R, Ketudat J, Cairns R, Akiyama T, Wara-Aswapati O, Savasti J, Esen A (2003) Characterization of a rice β-glucosidase highly expressed in flower and germinating shoot. Plant Sci 165:627–638. https://doi.org/10.1016/S0168-9452(03)00235-8

Qi X, Liu C, Song L, Li Y, Li M (2017) *PaCYP78A9*, a Cytochrome P450, regulates fruit size in sweet cherry (*Prunus avium* L.). Front Plant Sci 8:2076. https://doi.org/10.3389/fpls.2017.02076

Riechmann JL, Heard J, Martin G, Reuber L, Jiang C-Z, Keddie J, Adam L, Pineda O, Ratcliffe OJ, Samaha RR, Creelman R, Pilgrim M, Broun P, Zhang JZ, Ghandehari D, Sherman BK, Yu G-L (2000) *Arabidopsis* transcription factors: genome-wide comparative analysis among eukaryotes. Science 290:2105–2110. https://doi.org/10.1126/science.290.5499.2105

Sabatino L, Iapichino G, D'Anna F, Eristanna P, Giuseppe M, Giuseppe LR (2018) Hybrids and allied species as potential rootstocks for eggplant: effect of grafting on vigour, yield and overall fruit quality traits. Sci Hortic 228:81–90. https://doi.org/10.1016/j.scienta.2017.10.020

Shi D, Wang D (2005) Effects of various salt-alkaline mixed stresses on *Aneurolepidium chinense* (Trin.) Kitag. Plant Soil 271:15–26. https://doi.org/10.1007/s11104-004-1307-z

Singh K, Foley RC, Oñate-Sánchez L (2002) Transcription factors in plant defense and stress responses. Curr Opin Plant Biol 5:430–436. https://doi.org/10.1016/s1369-5266(02)00289-3

The Gene Ontology Consortium (2019) The Gene Ontology Resource: 20 years and still GOing strong. Nucleic Acids Res 47:D330–D338. https://doi.org/10.1093/nar/gky1055

Vera-Sirera F, Gomez MD, Perez-Amador MA (2016) DELLA proteins, a group of GRAS transcription regulators that mediate gibberellin signaling. In Gonzalez DH (ed) Plant transcription

factors. Academic Press, Boston, pp 313–328. https://doi.org/10.1016/B978-0-12-800854-6.00020-8

Wang C, Gao C, Wang L, Zheng L, Yang C, Wang Y (2014) Comprehensive transcriptional profiling of NaHCO$_3$-stressed *Tamarix hispida* roots reveals networks of responsive genes. Plant Mol Biol 84:145–157. https://doi.org/10.1007/s11103-013-0124-2

Wang YX, Hu Y, Zhu YF, Baloch AW, Jia XM, Guo AX (2018) Transcriptional and physiological analyses of short-term iron deficiency response in apple seedlings provide insight into the regulation involved in photosynthesis. BMC Genomics 19:461–472. https://doi.org/10.1186/s12864-018-4846-z

Wu B, Hu Y, Huo P, Zhang Q, Chen X, Zhang Z (2017) Transcriptome analysis of hexaploid hulless oat in response to salinity stress. PLoS ONE 12:e0171451. https://doi.org/10.1371/journal.pone.0171451

Xie M, Chen H, Huang L, O'Neil RC, Shokhirev MN, Ecker JR (2018) A B-ARR-mediated cytokinin transcriptional network directs hormone cross-regulation and shoot development. Nat Commun 9:1604. https://doi.org/10.1038/s41467-018-03921-6

Xu J, Wang XY, Guo WZ (2015) The cytochrome P450 superfamily: key players in plant development and defense. J Integr Agric 14:1673–1686. https://doi.org/10.1016/S2095-3119(14)60980-1

Xu M, Zeng CB, He R, Yan Z, Qi Z, Xiong R, Cheng Y, Wei SS, Tang H (2019) Transcriptome analysis of banana (*Musa acuminate* L.) in response to low-potassium stress. Agronomy 9: 169. https://doi.org/10.3390/agronomy9040169

Xu N, Liu S, Lu Z, Pang S, Wang L, Wang L, Li W (2020) Gene expression profiles and flavonoid accumulation during salt stress in *Ginkgo biloba* seedlings. Plants 9:1162. https://doi.org/10.3390/plants9091162

Yang JY, Zheng W, Tian Y, Wu Y, Zhou DW (2011) Effects of various mixed salt-alkaline stresses on growth, photosynthesis, and photosynthetic pigment concentrations of *Medicago ruthenica* seedlings. Photosynthetica 49:275–284. https://doi.org/10.1007/s11099-011-0037-8

Ye X, Wang H, Cao X, Jin X, Cui F, Bu Y, Liu H, Wu W, Takano T, Liu S (2019) Transcriptome profiling of *Puccinellia tenuiflora* during seed germination under a long-term saline-alkali stress. BMC Genomics 20:589. https://doi.org/10.1186/s12864-019-5860-5

Zhang M, Hong L, Gu M, Wu C-D, Zhang G (2020) Transcriptome analyses revealed molecular responses of *Cynanchum auriculatum* leaves to saline stress. Sci Rep 10:449. https://doi.org/10.1038/s41598-019-57219-8

Zhu Y, Wu Y, Hu Y, Jia X, Zhao T, Cheng L, Wang Y (2019) Tolerance of two apple rootstocks to short-term salt stress: Focus on chlorophyll degradation, photosynthesis, hormone and leaf ultra-structures. Acta Physiol Plant 41:87. https://doi.org/10.1007/s11738-019-2877-y